Biochimica et Biophysica Acta 1783 (2008) 1503–1516

Contents lists available at ScienceDirect

Biochimica et Biophysica Acta

journal homepage: www.elsevier.com/locate/bbamcr

Stimulation- and palmitoylation-dependent changes in oligomeric conformation of serotonin 5-HT1A receptorsi

Fritz Kobe [a,b,1], Ute Renner [a,b,1], Andrew Woehler [a], Jakub Wlodarczyk [a,d], Ekaterina Papusheva [b], Guobin Bao [a], Andre Zeug [a,c], Diethelm W. Richter [a,b], Erwin Neher [a,d], Evgeni Ponimaskin [a,b,*]

[a] DFG-Research Center for the Molecular Physiology of the Brain (CMPB), University of Göttingen, Germany
[b] Department Neuro- and Sensory Physiology, University of Göttingen, Germany
[c] Department Neurophysiology and Cellular Biophysics, University of Göttingen, Germany
[d] Max-Planck Institute for Biophysical Chemistry Göttingen, Germany

ARTICLE INFO

Article history:
Received 13 December 2007
Received in revised form 21 February 2008
Accepted 25 February 2008
Available online 12 March 2008

Keywords:
Oligomerization
Serotonin
G-protein coupled receptors
Palmitoylation
Foerster resonance energy transfer

ABSTRACT

In the present study we analyzed the oligomerization state of the serotonin 5-HT1A receptor and studied oligomerization dynamics in living cells. We also investigated the role of receptor palmitoylation in this process. Biochemical analysis performed in neuroblastoma N1E-115 cells demonstrated that both palmitoylated and non-palmitoylated 5-HT1A receptors form homo-oligomers and that the prevalent receptor species at the plasma membrane are dimers. A combination of an acceptor-photobleaching FRET approach with fluorescence lifetime measurements verified the interaction of CFP- and YFP-labeled wild-type as well as acylation-deficient 5-HT1A receptors at the plasma membrane of living cells. Using a novel FRET technique based on the spectral analysis we also confirmed the specific nature of receptor oligomerization. The analysis of oligomerization dynamics revealed that apparent FRET efficiency measured for wild-type oligomers significantly decreased in response to agonist stimulation, and our combined results suggest that this decrease was mediated by accumulation of FRET-negative complexes rather than by dissociation of oligomers to monomers. In contrast, the agonist-mediated decrease of FRET signal was completely abolished in oligomers composed by non-palmitoylated receptor mutants, demonstrating the importance of palmitoylation in modulation of the structure of oligomers.

1. Introduction

Until recently, G-protein coupled receptors were assumed to exist and function as monomeric entities that interact with the corresponding G-protein at a 1:1 stoichiometry. However, biochemical, structural and functional evidence obtained in the last decade suggests that some GPCRs can form homo- and hetero-oligomers [1]. Initial clues for the existence of receptor dimers and oligomers came from the appearance of high molecular weight SDS-resistant complexes on SDS-PAGE [2]. In addition, trans-complementation assays not only confirmed the existence of receptor–receptor interactions but also specified their functional implications. In these experiments, it was demonstrated that co-expression of two mutant receptors, which were not able to transduce signals individually, restored signal transduction [3,4]. Recently, GPCR dimers were directly visualized under physiological conditions when rhodopsin dimers in murine rod outer segments were imaged by atomic force microscopy [5]. Dimers were also found in crystal structure of rhodopsin [6].

Although there is evidence suggesting that oligomeric complexes may represent the preferred state of GPCRs [7], no general principle defining the regulation of oligomerization has been elucidated. There are two general models describing the mechanisms of GPCR oligomerization. One model proposes that GPCR oligomers are formed early after receptor synthesis and that oligomeric state does not change upon ligand treatment [8]. A well-known example of such constitutive oligomerization is the $GABA_BB$ receptor, for which oligomerization between $GABA_BR1$ and $GABA_B2$ has been shown to be necessary for the proper trafficking and functioning at the cell surface [9–11]. The other model, which has been documented for several GPCRs by using biochemical as well as biophysical approaches describes receptor oligomerization as a ligand-dependent process [12,13].

A variety of biochemical, functional and biophysical techniques has been utilized to demonstrate the existence of receptor complexes within the GPCR family. Cross-linking and co-immunoprecipitation assays represent classical methods for the analysis of GPCR oligomerization. However, these methods are not applicable to living cells and therefore can not provide information about the dynamic changes upon agonist stimulation. An additional drawback is that the biochemical treatment could possibly result in artificial receptor aggregation. The development

* Corresponding author. Tel.: +49 551 397097; fax: +49 551 396031.
E-mail address: eponima@gwdg.de (E. Ponimaskin).
[1] Authors contributed equally to this paper.

0167-4889/$ – see front matter © 2008 Elsevier B.V. All rights reserved.
doi:10.1016/j.bbamcr.2008.02.021

of new approaches, such as Förster Resonance Energy Transfer (FRET) techniques either based on fluorescence or on bioluminescence was therefore essential for the studies of GPCR oligomerization under physiological conditions [14]. FRET signals can be obtained when an acceptor fluorophore is located within close enough proximity of an excited donor fluorophore to initiate a dipole-dipole interaction, which can result in a non-radiative energy transfer from the donor to the acceptor fluorophore. This non-radiative transfer of energy can occur only when (*i*) the donor possesses an emission spectra overlapping with the excitation spectra of the acceptor, [4] (*ii*) both fluorophores are located within 1 to 10 nm of each other and (*iii*) their transition dipole moments are appropriately oriented [15].

In this study, we examined the oligomerization state of the serotonin 5-HT1A receptor and analyzed its dynamics in living cells. The 5-HT1A receptor can couple to a variety of effectors via the pertussis-toxin sensitive heterotrimeric G-proteins of the Gi/o families [16–18] and is the most extensively characterized member of the serotonin receptor family. Activation of the 5-HT1A receptor results in the inhibition of adenylate cyclase and subsequent decrease of intracellular cAMP levels. In addition to the effects mediated by the Gαi/o subunit, activation of the 5-HT1A receptor leads to a Gβγ-mediated activation of a K^+ current, inhibition of a Ca^{2+} current, stimulation of the phospholipase C, as well as an activation of the mitogen-activated protein kinase Erk2 [19–22]. With respect to its physiological functions, it is noteworthy that the 5-HT1A receptor is involved in manifold processes including the regulation of neurogenesis [23], respiratory control [24,25], cardiovascular control [26], neuroendocrine regulation [27], temperature control [28] and regulation of sleep [29]. Considerable interest in this receptor has been raised due to its involvement in regulation of depression and anxiety states [28,30,31].

Previously, we have demonstrated that the 5-HT1A receptor is stably palmitoylated at its C-terminal cysteine residues Cys417 and Cys420. Characterization of acylation-deficient 5-HT1A mutants revealed that palmitoylation of the 5-HT1A receptor is critical for G_i-protein coupling and effector signaling [32]. The covalent attachment of palmitic acid to the cysteine residue(s) located within the C-terminus represents a very common post-translational modification of GPCRs [33]. Moreover, palmitoylation of several GPCRs has been shown to play a central role in the regulation of the receptor's functions. Recent studies on rhodopsin indicate that its depalmitoylation enhances light-dependent GTPase activity of G_t and strongly decreases the light-independent activity of opsin-*atr* [22,34]. The functional characterization of non-palmitoylated β2-adrenergic and endothelin-B (ET_B) receptors has revealed that palmitoylation is essential for agonist-stimulated coupling to G_s and to both G_q- and G_i-proteins, respectively [35–37]. Analysis of the non-palmitoylated ET_A receptor mutant demonstrated that ligand-induced stimulation of G_s was unaffected by the lack of palmitoylation, whereas signaling through G_q was prevented [36]. Recent data on chemokine CCR5 and prostacyclin receptors also demonstrated that receptor palmitoylation is involved in the activation of intracellular signaling pathways [38,39].

All receptors mentioned above have also been found to undergo oligomerization. However, the relationship between receptor palmitoylation and oligomerization has not yet been investigated. Therefore, in the present study, in addition to providing evidence for oligomerization of wild-type 5-HT1A receptors, we investigate whether a palmitoylation state of 5-HT1A receptor may affect its oligomerization.

2. Materials and Methods

2.1. Recombinant DNA procedures

The construction of HA-tagged 5-HT1A and 5-HT1A receptors fused to different spectral variants of the green fluorescence proteins as well as their palmitoylation-deficient counterparts has been described previously [32,40]. The plasmids encoding for Gαi2, Gβ1 and Gγ2 subunits of heterotrimeric G-protein from mice were kindly provided by Dr. Tatyana Voyno-Yasenetskaya (University of Illinois, Chicago).

2.2. Adherent cell culture and transfection

Mouse N1E-115 neuroblastoma cells from the American Type Culture collection (ATCC) were grown in Dulbecco's modified Eagle's medium (DMEM) containing 10% fetal calf serum (FCS) and 1% penicillin/streptomycin at 37 °C under 5% CO_2. For transient transfection, cells were seeded at low-density in 60-mm dishes (1×10^6) or on 10-mm cover-slips (5×10^5) and transfected with appropriate vectors using Lipofectamine2000 Reagent (Invitrogen) according to the manufacturer's instruction. Four hours after transfection, cells were serum starved over night before analysis.

The amount of expressed receptor was measured in membrane preparations of transfected cells by using radioactive ligand binding assay with [^{3}H]8-OH-DPAT as a specific ligand and non-radioactive 5-HT as a competitor.

2.3. Immunoprecipitation and immunoblotting

Twenty-four hours post-transfection cells were washed in PBS and lysed in 500 µl RIPA-buffer (20 mM Tris–HCl pH 7.4, 150 mM NaCl, 10 mM EDTA, 10 mM iodacetamide, 1% Triton X-100, 1% deoxycholic acid, 0.1% SDS, 1 mM PMSF, 5 µg/ml aprotinin, 2 µg/ml leupeptin) for 30 min on ice. The lysate was cleared by centrifugation at 13.000 rpm for 20 min at 4 °C. The receptors were immunoprecipitated from the supernatant by incubation with rabbit anti-HA antibody (Santa Cruz) or anti-GFP antibody (Abcam) for 4 h at 4 °C, followed by incubation of lysates with protein A-sepharose (Sigma) for 2 h. The immunoprecipitation-sepharose complexes were washed with RIPA-buffer, eluted with 40 µl Laemmli loading buffer, and 15 µl of each sample were separated by 10% SDS-PAGE under reducing conditions. Proteins were transferred to Hybond nitrocellulose membrane (Amersham) and probed either with antibodies against HA-tag (Santa Cruz; 1:5000 diluted in PBS/Tween20) or against GFP (Eusera; diluted 1:20.000 in PBS/Tween20). Proteins were detected using the AceGlow detection reagents (Peqlab).

2.4. Chemical cross-linking

Transiently transfected cells were resuspended in PBS (150 mM NaCl, 20 mM NaH_2PO_4, pH 7.4) and mixed with the indicated concentrations of cross-linker 1,11-bis-Maleimidotriethyleneglycol ($BM[PEO]_3$, Pierce) diluted in PBS for 10 min at room temperature. The reaction was stopped by addition of dithiothreitol to a final concentration of 10 mM followed by incubation on ice for 10 min. After two washes with PBS, cells were lysed and proteins were immunoprecipitated and subjected to the SDS-PAGE and immunoblot analysis.

2.5. Confocal imaging and single-cell acceptor-photobleaching FRET analysis

Images of N1E-115 cells expressing 5-HT1A-CFP and 5-HT1A-YFP fusion proteins were acquired with an LSM510-Meta confocal microscope (Carl Zeiss Jena) equipped with a 40×/1.3 NA oil- immersion objective at 512×512 pixels. The 458 nm line of a 40 mW argon laser was used at 15% power. Fluorescence emission was acquired from individual cells over fourteen lambda channels, at 10.7 nm steps, ranging from 475 to 625 nm. For each measurement a series of 8 images was acquired over a duration of 124 s. After the 4th image acquisition, bleaching of the acceptor (YFP) was performed in a selected 20×20 pixel region of interest in the plasma membrane. For that the 514 nm line of the Argon laser set at 50% power and 100% transmission for 300 scanning interactions using a 458nm/514nm dual dichroic mirror was used. Linear unmixing was performed by the Zeiss AIM software package using CFP and YFP reference spectra obtained from images of cells expressing only 5-HT1A-CFP or 5-HT1A-YFP acquired with acquisition settings mentioned above. Apparent FRET efficiency was calculated offline using the equation,

$$Ef_D = 1 - \left(\frac{F_{DA}}{F_D}\right) \quad (1)$$

where f_D is the fraction of donor participating in the FRET complex (i.e. ratio of FRET complexes over a total donor concentration, $[DA]/[D^t]$), F_{DA} and F_D are the background subtracted and acquisition bleaching corrected pre- and post-bleach CFP fluorescence intensities, respectively. The acquisition bleaching corrected post-bleach CFP intensities were calculated as

$$F_D = F_D^{B,post} + \left(\frac{F_D^{R,pre} - F_D^{R,post}}{F_D^{R,pre}}\right) F_D^{B,pre} \quad (2)$$

where F_D^B and F_D^R refer to CFP intensities of the bleach and reference region of interest, and *pre* and *post* refer to pre-bleach and post-bleach measurements.

2.6. Spectral FRET analysis in living cells

Mouse N1E-115 neuroblastoma cells were co-transfected with plasmid DNAs encoding for wild-type and/or acylation-deficient 5-HT1A receptors fused with CFP and YFP. Sixteen hours after transfection, cells were resuspended in PBS. All measurements

were performed in 5 mm pathway quartz cuvettes using a spectrofluorometer (Fluorolog, Horiba JobinYvon) equipped with xenon lamp (450 W, 950 V). The cell suspension was stirred with a magnetic stirrer while the temperature was maintained at 37 °C during the experiment.

For calibration measurements, cells were co-transfected with plasmid encoding a single fluorophore- tagged 5-HT1A receptor together with an equal amount of plasmid encoding HA-tagged 5-HT1A receptor. During the time-course experiments, two emission spectra were obtained for each time point by exciting at 458 nm and 488 nm with 5 nm spectral resolution for excitation and emission and 0.5 s integration time. The spectral contributions due to light scattering and non-specific fluorescence of the cells were taken into account by subtracting the emission spectra of non-transfected cells (background) from each measured spectra. Before each measurement, the spectrofluorometer was calibrated for the xenon-lamp spectrum and Raman scattering peak position. Stimulation of 5-HT1A receptors was carried out using serotonin (Sigma) at a final concentration of 10 μM. For antagonist treatment, WAY 100135 (Tocris) at a final concentration of 1 μM was used. Cholesterol depletion was carried out by treating cells with 2% methyl-ß-cyclodextrin (MßCD) in serum-free D-MEM for 45 min at 37 °C.

2.7. Apparent FRET efficiency calculations

To determine changes in apparent FRET efficiency due to 5-HT1A receptor activation by serotonin we used a recently developed method described in detail by Wlodarczyk et al. [41]. Calibration measurements were carried out with cells expressing only donor [D^{ref}] (5-HT1A-CFP) or acceptor [A^{ref}] (5-HT1A-YFP) using two excitation wavelengths λ^i (i=1,2) as described in the previous section.

Calibration measurements allowed us to obtain the concentration related extinction coefficient ratio ($r^i=\varepsilon^i_D[D^{ref}]/\varepsilon^i_A[A^{ref}]$). This was done by fitting the curve resulting from acceptor reference spectra multiplied by the quantum yield and emission characteristics of the donor (i.e. emission spectra normalized to unit area) to that of donor reference spectra multiplied by the quantum yield, and emission characteristics of the acceptor [41].

We also performed reference measurements with cells co-expressing 5-HT1A-CFP and 5-HT1A-YFP receptors. Combinations of the acceptor and donor reference spectra were fitted to the measured spectra of cells co-expressing 5-HT1A-CFP and 5-HT1A-YFP and the apparent relative acceptor and donor concentrations α^i and δ^i, respectively, were obtained as the weights of those fits. The quantities α^i, δ^i obtained together with two scaling factors (r^i) reflecting the excitation ratios of two fluorophores at a given excitation wavelength λ^i, allow for a calculation of the total concentration ratio [A^t]/[D^t] of donor and acceptor as well as the apparent FRET efficiencies Ef_A and Ef_D, where f_A and f_D are the fractions of acceptors and donors in complexes.

$$Ef_D \equiv E\frac{[DA]}{[D^t]} = 1 - \frac{r^{ex,1} + R^t}{r^{ex,1} + \alpha^1/\delta^1} \text{ and} \tag{3}$$

$$Ef_A \equiv E\frac{[DA]}{[A^t]} = \frac{[D^{ref}]}{[A^{ref}]}\frac{\Delta\alpha}{\alpha^1 r^{ex,2} - \alpha^2 r^{ex,1}}, \tag{4}$$

where R^t is a concentration ratio calculated as,

$$R^t \equiv \frac{[A^t][D^{ref}]}{[D^t][A^{ref}]} = \frac{\alpha^1 r^{ex,2} - \alpha^2 r^{ex,1}}{\Delta r\delta^1 + \Delta\alpha} \tag{5}$$

with the definitions $\Delta\alpha=\alpha^1-\alpha^2$ and $\Delta r=r^{ex,1}-r^{ex,2}$. Where $f_D \equiv [DA]/[D^t]$ and $f_A \equiv [DA]/[A^t]$ representing the fractions of donor and acceptor participating in complexes.

2.8. Analysis of specific vs. random receptor–receptor interactions

In order to distinguish between receptors interacting randomly from those with specific interaction, apparent FRET efficiencies were obtained for various acceptor to donor ratios by keeping the total concentration of fluorophores constant. It has been proposed that the dependency of Ef_D on [A^t]/[D^t] for dimers differs from that of Ef_D resulting from random interaction [42]. The apparent FRET efficiency Ef_D obtained from our experimental data was plotted as a function of the total acceptor to donor ratio [A^t]/[D^t] and fitted by least square minimization to the following equation, as proposed previously by Veatch and Stryer [42] and later modified by James et al [43] to the form

$$Ef_D = \left(1 - \frac{1}{\left(1+[A^t]/[D^t]\right)}\right)E, \tag{6}$$

where E is the characteristic FRET efficiency. It is also notable, that the above equation was derived for the case of high-affinity dimerization reaction [42].

2.9. Fluorescence lifetime FRET measurements

Fluorescence intensity decays were obtained by time-correlated single photon-counting measurements of fluorescence using a Fluorolog-3 spectrofluorometer (Horiba Jobin Yvon, München, Germany). Samples were placed in 10-mm pathway quartz cuvettes (10×10 mm^2) and continuously stirred with a magnetic stirrer. Emission was collected in right angle geometry. Excitation was performed with a 460 nm nanoLED with a 440/40 nm transmission filter (Semrock, Tuebingen, Germany). Fluorescence intensity was measured in the wavelength band from 468 nm to 482 nm to avoid acceptor fluorescence. Typical fluorescence decays were fitted with the resulting sum of one, two, or three exponentials, interatively convolved with the instrument response function using the standard DataStation analysis software provided by Horiba Jobin Yvon and CFS_LS software (available from Center for Fluorescence Spectroscopy at http://cfs.umbi.umd.edu/cfs/software/). The quality of the fits was evaluated by the structure observed in the plots of residuals and by the reduced chi-square values. The mean fluorescence lifetimes were calculated as the amplitude-weighted life-times. In several experiments cholesterol depletion was carried out by treating cells with 2% methyl-β-cyclodextrin (MßCD) in serum-free D-MEM for 45 min at 37 °C before the analysis.

2.10. Gradient centrifugation

Separation of detergent-resistant membranes derived from transfected N1E-115 cells (1×10^6) growing on 35 mm dishes was performed as recently described [40]. Cells were lysed in TNE buffer (25 mM Tris–HCl, pH7.4, 150 mM NaCl, 5 mM EDTA, 1 mM DTT, 10% sucrose, 1% Triton X-100, 1 mM PMSF, 10 μM Leupeptin, 2 μg/ml Aprotinin) and lysates (1.2 mg protein/ml) were mixed with the double volume of 60% Optiprep™ gradient medium (Sigma). The resulting 40% Optiprep™ mixture was transferred into the ultracentrifuge tube and overlaid with steps of each 35%, 30%, 25%, 20% and 0% Optiprep™ in TNE. The gradients were centrifuged for 5 h at 50.000 rpm in the TLS-55 rotor of the ultracentrifuge TL-100 (Beckman). Six fractions were collected from the top of the gradient and TCA-precipitated. The protein pellets were analyzed by SDS-PAGE followed by immunoblot analysis with appropriate antibodies. In several experiments chemical cross-linking with $BM[PEO]_3$ together with 5-HT treatment (10 μM) was performed before ultracentrifugation.

3. Results

3.1. Biochemical analysis of 5-HT1A receptor oligomerization

In order to determine whether the 5-HT1A receptor undergoes oligomerization, we applied a co-immunoprecipitation assay to N1E-115 mouse neuroblastoma cells co-expressing HA- and YFP-tagged receptors. The HA-tagged 5-HT1A receptor has a molecular weight of approximately 48 kDa (Fig. 1, upper panel), while the molecular weight of YFP-tagged receptors is shifted to 74 kDa (Fig. 1, lower panel). Fig. 1A also shows that after immunoprecipitation with an antibody against HA-tag, YFP- immunoreactive receptor bands were identified only in samples derived from cells co-expressing both HA- and YFP-tagged receptors. Equal results were obtained after initial immunoprecipitation of cell lysates with an anti-YFP antibody followed by immunoblotting with an anti-HA-tag antibody (Fig. 1A). To exclude the possibility that the identified bands represent artificial protein aggregates, cells expressing only one type of receptor (HA- or YFP-tagged) were mixed prior to lysis and analyzed in parallel as a control. As shown in Fig. 1, individual receptors can be precipitated and detected by the same antibody, whereas co-immunoprecipitation did not occur, supporting specificity of 5-HT1A receptor oligomerization.

We have recently shown that the 5-HT1A receptor is modified by covalently attached palmitate [32] Therefore, we analyzed the impact of palmitoylation on receptor oligomerization. Fig. 1B and C demonstrate that differently tagged 5-HT1A receptors were efficiently co-immunoprecipitated independently of their acylation state.

To investigate 5-HT1A receptor oligomerization in a physiological environment, N1E-115 cells expressing either wild-type or acylation-deficient HA-tagged receptors were treated with chemical cross-linker $BM[PEO]_3$. This homobifunctional cross-linker interacts with sulfhydryl groups on polypeptides to form stable thioether linkages that induces an irreversible cross-linking of proteins located within close proximity (approximately 15 Å) of each other. It is notable that the plasma membrane is impermeable for $BM[PEO]_3$, allowing oligomerization analysis of the receptors localized on the cell surface of intact cells. Immunoblotting analysis of N1E-115 cells expressing the wild-type or the palmitoylation-deficient receptors revealed that, in the absence of cross-linker, the majority of 5-HT1A receptors is detectable as monomers, while only a minor fraction migrates as a

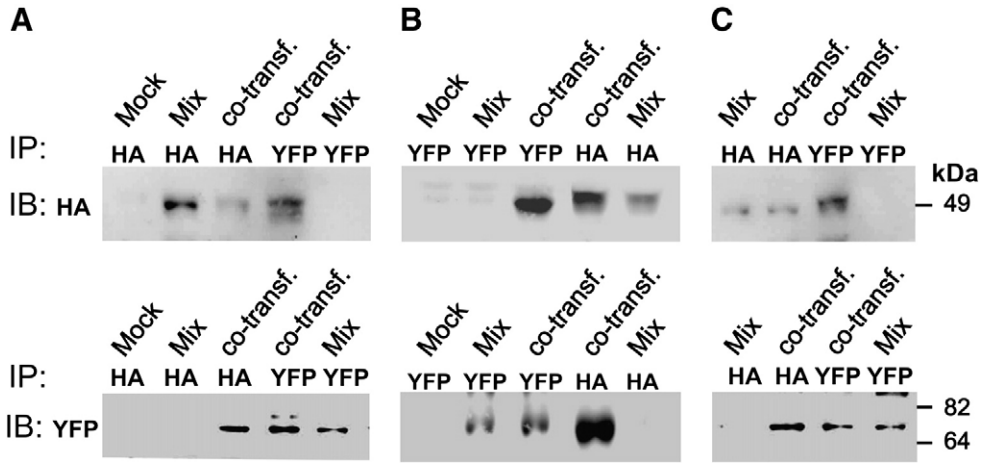

Fig. 1. Analysis of 5-HT1A receptor oligomerization by co-immunoprecipitation. Interactions between HA- and YFP-tagged wild-type receptors (A), palmitoylation-deficient mutants (B) as well as YFP-tagged wild-type and HA-tagged palmitoylation-deficient receptors (C) were analyzed. Neuroblastoma N1E-115 cells co-expressing HA- and YFP-tagged receptors (*co-transf.*), a mixture of cells expressing each receptor individually (*Mix*) or non-transfected cells (*Mock*) were subjected to immunoprecipitation followed by SDS/PAGE (10%) and immunoblot. IP refers to the antibodies used for immunoprecipitation, while IB defines the antibody used for immunoblot. The immunoblots shown are representative of at least 4 independent experiments.

band with molecular weight of app. 95 kDa, which is the molecular weight predicted for a dimer (Fig. 2A). Treatment of intact cells with increasing concentrations of cross-linker leads to a decline of the amount of monomers that is accompanied by an increase in the dimer population. Similar results were also obtained for the acylation-deficient mutant (Fig. 2B).

To analyze effect of agonist stimulation on receptor oligomerization, N1E-115 cells expressing wild-type or acylation-deficient 5-HT1A receptors were treated with 5-HT at 10 μM concentration followed by co-immunoprecipitation or cross-linking analysis. Fig. 3A demonstrates that stimulation of either wild-type or non-palmitoylated receptors with agonist does not change amount of co-immunoprecipitated receptors. Similar results were also obtained after application of cross-linker BM[PEO]$_3$ to the simulated and non-stimulated cells (Fig. 3B), demonstrating that the oligomerization state of 5-HT1A receptor is not modulated upon agonist stimulation.

3.2. Acceptor-photobleaching analysis of 5-HT1A receptor oligomerization

Förster Resonance Energy Transfer (FRET) is a powerful biophysical approach for the quantitative analysis of protein-protein interactions [15]. To determine whether FRET could be measured in the plasma membrane of living cells co-expressing 5-HT1A-CFP and 5-HT1A-YFP fusion proteins, a confocal microscopy-based acceptor-photobleaching method was applied to transfected N1E-115 cells.

To avoid artefacts resulting from overexpression, we adjusted the total expression level for the CFP- and YFP-tagged receptor to 1.000–1.200 fmol/mg proteins in all following FRET experiments, which allows for quantitative analysis of results obtained in different experiments. Moreover, similar amounts of endogenous 5-HT1A receptors has been obtained in hippocampus under physiological conditions [44,45].

CFP and YFP were excited simultaneously with a 458 nm laser line. Fluorescence emission was acquired at multiple wavelengths using the LSM510-Meta detector allowing for the linear unmixing of the CFP and YFP emission spectra. Confocal microscopy performed after the transfection of N1E-115 cells revealed that the majority of YFP- and CFP-tagged 5-HT1A receptors were localized in the plasma membranes with only a minor fraction existing in the intracellular compartments (Fig. 4A).

To perform acceptor photobleaching, a defined region of plasma membrane was selectively illuminated using a 514 nm laser line. A 458/514 nm dual dichroic mirror was used to allow rapid image acquisition before and immediately after photobleaching. Fig. 4A shows the bleached region of interest with a loss of YFP intensity as well as a reference region of interest from which the acquisition bleaching rate was determined for correct FRET calculation. Fig. 4B

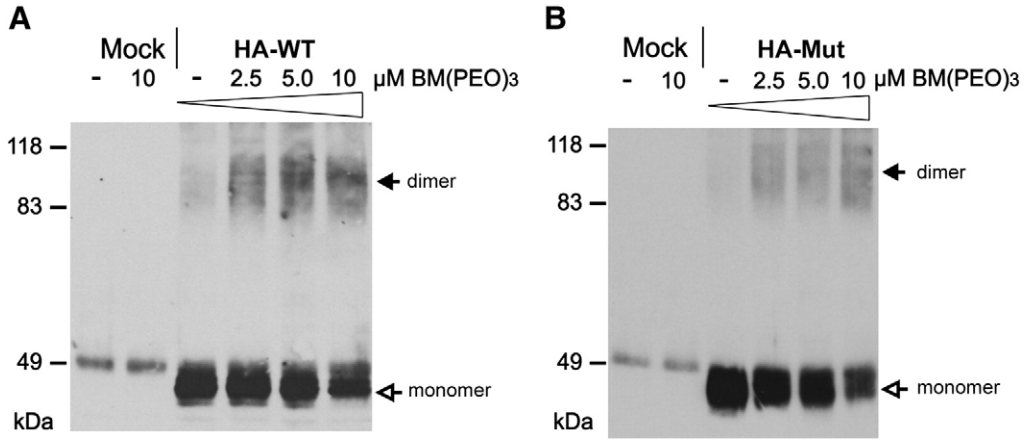

Fig. 2. Chemical cross-linking of wild-type and acylation-deficient 5-HT1A receptors. Intact N1E-115 cells expressing either HA-tagged wild-type (A) or mutant 5-HT1A receptors (B) were treated with increasing concentrations of cross-linker BM[PEO]$_3$ and subjected to immunoprecipitation, SDS/PAGE and immunoblot analysis with anti-HA antibody. Apart from the receptor monomers, species migrating with the expected size of a dimer are visible. The immunoblots shown are representative of at least 4 independent experiments.

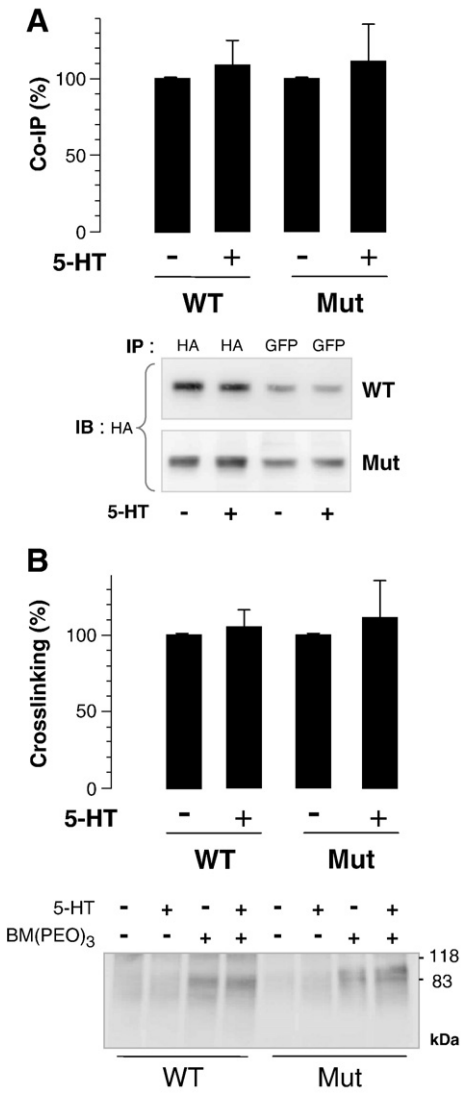

Fig. 3. Agonist stimulation does not change amount of 5-HT1A oligomers. (A) Neuroblastoma N1E-115 cells co-expressing HA- and YFP-tagged receptors were treated with 5-HT (10 μM) or with vehicle (PBS) for 15 min and then subjected to co-immunoprecipitation. The intensity of protein bands was assessed by densitometry of immunoblots. The value for PBS treated cells was set to 100%. Bars represent means + S.E.M. (n=3; top). The representative immunoblot is shown where IP refers to the antibodies used for immunoprecipitation, while IB defines the antibody used for immunoblot (bottom). WT, wild-type 5-HT1A receptor; Mut, acylation-deficient mutant. (B) N1E-115 cells expressing either HA-tagged wild-type or non-palmitoylated 5-HT1A receptors were treated with 5-HT (10 μM) or with vehicle (PBS) for 15 min with cross-linker $BM[PEO]_3$ (5 μM) and then subjected to immunoprecipitation and immunoblot analysis with anti-HA antibody. The intensity of protein bands corresponding to dimers was assessed by densitometry of immunoblots. The value for PBS and $BM[PEO]_3$ treated cells was set to 100%. Bars represent means + S.E.M. (n=3; top). A representative immunoblot is shown (bottom).

illustrates the changes in emission intensities of donor and acceptor fluorescence in the bleached region of interest demonstrating that with the loss of acceptor fluorescence there is a corresponding increase of donor emission intensity that is characteristic of FRET. In contrast, intensities of both CFP and YFP fluorescence of non-bleached regions undergo only minor decrease, reflecting acquisition bleaching (Fig. 4C).

Finally, apparent FRET efficiency Ef_D was calculated according to Eq. (1), where F_{DA} is the pre-bleach and F_D is the corrected post-bleach donor fluorescence according to Eq. (2). Data were background subtracted and corrected for acquisition bleaching using the measurements from the reference region of the plasma membrane (Fig. 4D). The wild-type receptor fusion proteins from cells with similar donor to acceptor ratios were found to have a mean apparent FRET efficiency of 16.4% ± 0.7%. For the negative controls obtained after co-transfection of cytosolic CFP and YFP an apparent FRET efficiency was 5.5% ± 3.8%. To examine whether oligomerization may depend on palmitoylation state of the receptor, we made acceptor-photobleaching trials in cells expressing non-palmitoylated mutants. The palmitoylation-deficient 5-HT1A receptors exhibited apparent FRET efficiency with a mean Ef_D of 23.6% ± 2.9%. In addition, we analyzed the interaction between wild-type receptors coupled to YFP and mutant receptors coupled to CFP. In this case a mean Ef_D value of 29.8% ± 5.6% was estimated. These results indicate that 5-HT1A forms oligomers and that the FRET efficiency depends on the palmitoylation status of the complex-forming units.

3.3. Analysis of receptor oligomerization by fluorescence lifetime FRET measurements

In addition to acceptor photobleaching, we quantified the FRET efficiency (E) in living cells by measuring fluorescence lifetime of tagged 5-HT1A receptors. N1E-115 cells were transfected either with 5-HT1A receptor fused to CFP or co-transfected with wild-type (WT) and acylation-deficient (Mut) receptors fused to CFP and YFP to create appropriate donor/acceptor pair at the ratio 1:1 in following combinations: WT-YFP/WT-CFP, Mut-CFP/Mut-YFP and WT-CFP/Mut-YFP. The fluorescence decays of donor fusion proteins were measured by time-correlated single photon counting (TCSPC) as described in Materials and Methods. Experimental decay curves were analyzed and mean value of fluorescence lifetime was calculated. The averaged fluorescence lifetime value calculated for CFP fused with receptor was found to be τ_D = 2.01 ± 0.05 ns. The decay kinetic of CFP in the cells expressing different receptor combinations were strongly affected by the presence of acceptor (YFP) leading to a shortening of the lifetime. Fluorescence lifetimes were found to be τ = 1.67 ± 0.11 ns, τ = 1.56 ± 0.16 ns and τ = 1.57 ± 0.2 ns for WT-CFP/WT-YFP, Mut-CFP/Mut-YFP and WT-CFP/Mut-YFP, respectively. FRET efficiency was calculated from these average lifetimes using the equation $E = 1 - \langle\tau\rangle_{TC}/\langle\tau\rangle_D$ and was determined to be E = 0.17 ± 0.04 for WT-CFP/WT-YFP, E = 0.22 ± 0.06 for Mut-CFP/Mut-YFP, E = 0.22 ± 0.05 for WT-CFP/Mut-YFP (Fig. 5). This confirms acceptor-photobleaching data and demonstrates that FRET efficiency for oligomers composed by acylation-deficent mutants as well as for mixed oligomers (i.e. combined by wild-type and mutant) is increased in comparison to the wild-type oligomers.

We have recently shown that a significant fraction of the 5-HT1A receptor resides in membrane rafts, while the yield of the palmitoylation-deficient receptor in these membrane microdomains is considerably reduced [40]. To analyze the role of lipid raft localization of 5-HT1A receptor for its oligomerization we measured the fluorescence lifetime after treatment of transfected cells with methyl-β-cyclodextrin (MβCD). The cholesterol-binding reagent MβCD was previously shown to disrupt the cholesterol-enriched membrane subdomains by depletion of cholesterol from the plasma membrane [46]. Destroying of lipid rafts resulted in shortening of fluorescence lifetime only in case of WT-CFP/WT-YFP (τ = 1.33 ± 0.05 ns), leading to significant increase of FRET value to E = 0.34 ± 0.02 (Fig. 5). In contrast, FRET efficiency calculated for Mut-CFP/Mut-YFP and WT-CFP/Mut-YFP was not affected by cholesterol depletion and was determined to be E = 0.22 ± 0.02 (τ = 1.56 ± 0.06 ns) and E = 0.16 ± 0.03 (τ = 1.68 ± 0.1 ns), respectively (Fig. 5).

3.4. Spectrometric detection of FRET between 5-HT1A receptors in living cells

We further examined FRET occurrence between fluorophore-labeled 5-HT1A receptors in living cells by analysis of emission spectra collected with a spectrofluorometer. Fig. 6 shows the typical fluorescence emission spectra at 420 nm excitation obtained in N1E-

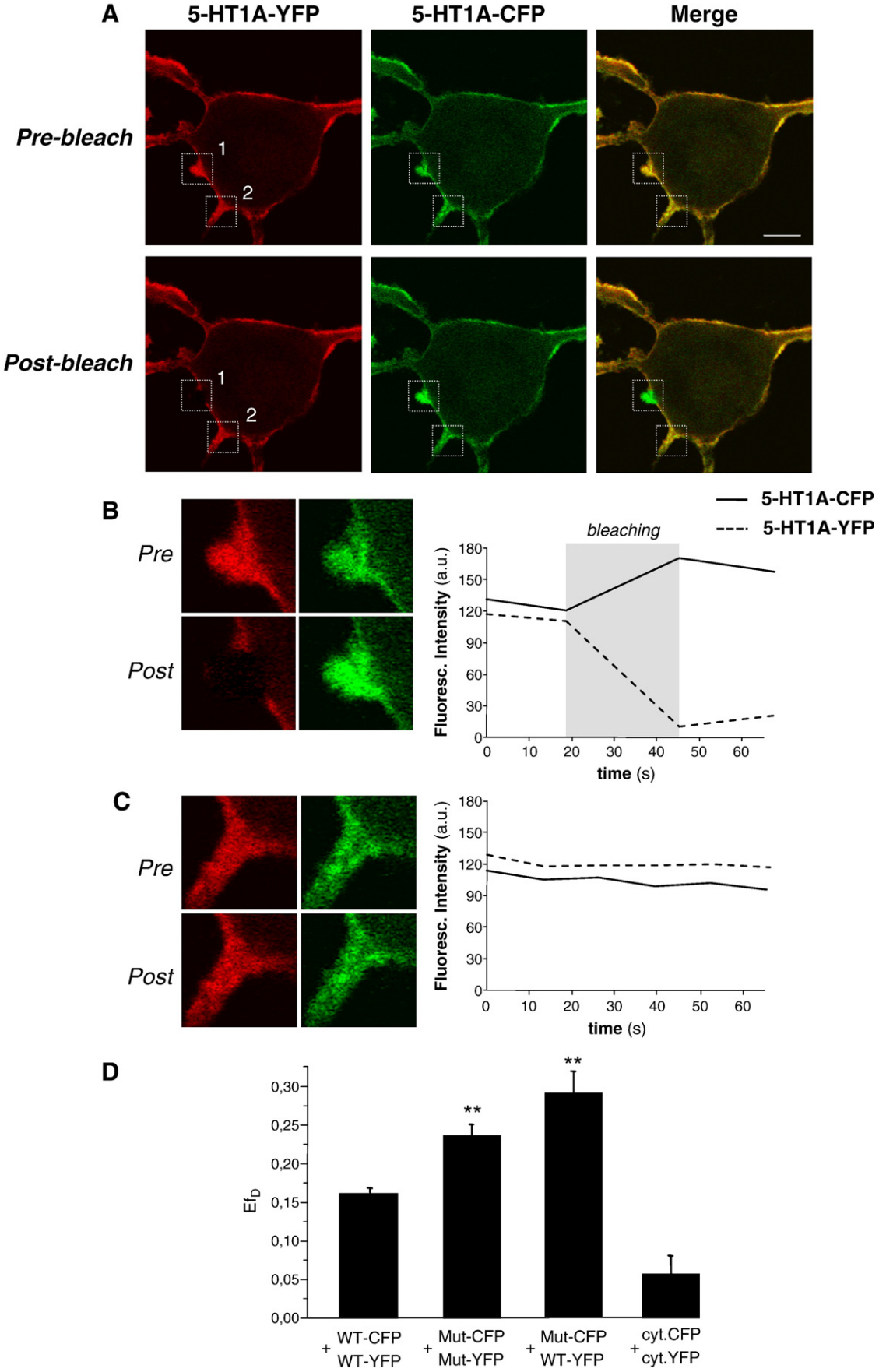
A
5-HT1A-YFP
5-HT1A-CFP
Merge
Pre-bleach
Post-bleach
1
2
B
Pre
Post
5-HT1A-CFP
5-HT1A-YFP
bleaching
Fluoresc. Intensity (a.u.)
time (s)
C
Pre
Post
Fluoresc. Intensity (a.u.)
time (s)
D
Ef_D
**
**
+ WT-CFP WT-YFP
+ Mut-CFP Mut-YFP
+ Mut-CFP WT-YFP
+ cyt.CFP cyt.YFP

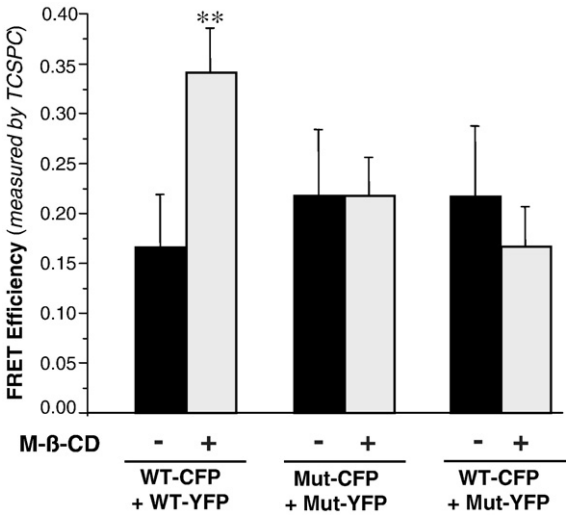

Fig. 5. Analysis of 5-HT1A oligomerization by fluorescence lifetime measurements. N1E-115 cells were co-transfected with wild-type (WT) and acylation-deficient (Mut) receptors fused to CFP and YFP in following combinations: WT-YFP/WT-CFP, WT-CFP/Mut-YFP and Mut- CFP/Mut-YFP. The co-transfected cells were treated with 10 mM MßCD for 45 min or were left untreated, and the averaged FRET efficiency values were calculated after fluorescence lifetime analysis as described in Materials and methods section. Data represent the means±S.E.M. ($n=3$). A statistically significant difference between the FRET efficiency obtained in cells co-expressing WT- CFP/WT-YFP before and after cholesterol depletion is shown (**, $p<0.01$).

115 cells expressing WT-CFP, WT-YFP or co-expressing WT-CFP and WT-YFP as a FRET pair. The spectral contaminations due to light scattering and nonspecific fluorescence of cells were taken into account by subtracting the emission spectra of HA-tagged receptor cells (background) from each measured spectra. When cells were transfected with only CFP-fused receptor, the typical emission spectrum of CFP with emission peaks at 475 nm and 500 nm was obtained (Fig. 6A). The emission spectrum obtained for cells expressing only YFP-fused receptor was similar to that obtained in HA-tagged receptor cells with only a very weak peak at 525 nm. In contrast, cells co-expressing WT-CFP and WT-YFP receptors demonstrated a significantly larger emission peak at 525 nm concomitant with a smaller CFP emission, which demonstrates the energy transfer from CFP to YFP (Fig. 6A). Similar results were also obtained when cells were co-transfected with acylation-deficient 5-HT1A mutant (Fig. 6B). This data confirms the oligomerization of 5-HT1A receptors in living cells.

3.5. Specificity of 5-HT1A receptor oligomerization

The apparent FRET efficiency, Ef_D, measured by acceptor photobleaching is inherently dependent on f_D, the fraction of donor participating in FRET complexes. This is in turn dependent upon the ratio of intact donor concentration to intact acceptor concentration present in the sample. It has been therefore suggested that the dependence of Ef_D on $[A^t]/[D^t]$ may be useful in differentiating FRET resulting from specific vs. random interactions [43,47,48]. In the case of random interaction, Ef_D has been predicted to be independent of the total donor to acceptor ratio at a fixed surface density above a certain ratio.

For receptor dimers, Ef_D values are expected to be dependent on the relative donor concentration at a higher $[A^t]/[D^t]$ threshold, resulting in a higher asymptotic Ef_D value. To analyze whether the measured apparent FRET efficiency reflects specific receptor–receptor interaction or resulted from random molecular interaction, Ef_D values were measured over a range of acceptor to donor ratios, wherein the combined concentration of plasmids encoding for donor and acceptor was held constant. Fig. 7A shows Ef_D values obtained for wild-type 5-HT1A receptors plotted against the $[A^t]/[D^t]$ ratio. As a negative control we used co-transfections of non-interacting cytosolic CFP and YFP proteins. Ef_D values obtained for cytosolic CFP and YFP and the corresponding $[A^t]/[D^t]$ ratio were fitted according to Eq. (6). Evaluation of the fit quality clearly shows that data obtained from the co-transfected cytosolic CFP/YFP ($R^2=0.37$) cannot be properly characterized by a model assuming specific oligomerization. This demonstrates that detected FRET resulted from non-specific, random interactions. Using this as a negative control for oligomerization, we analyzed the data collected for the cells co-transfected with 5-HT1A-CFP and 5-HT1A-YFP receptors. In this case, we found that Ef_D values were substantially higher (Fig. 7A), and Eq. (6) provides a very good fit quality of Ef_D data ($R^2=0.90$). Furthermore, in a proper fit to the proposed model, experimentally measured Ef_D value at a donor/acceptor ratio of 1:1 should represent half of the asymptotic value for Ef_D. In the case of receptor we found that the Ef_D values at a ratio of 1:1 was approximately 0.12, which corresponds to the obtained asymptotic value for the fit of approximately $Ef_D=0.24$ (Fig. 7A). In contrast, the Ef_D value measured for co-transfected CFP and YFP at a ratio of 1:1 was equal to 0.025, which is a clear underestimate when compared to the fitted curve (Fig. 7A). Similar results were also obtained after analysis of Ef_A values (Fig. S1) and for cells co-transfected with Mut-CFP/WT-YFP and Mut- CFP/Mut-YFP combinations (data not shown).

Interaction specificity may also be analyzed by plotting energy transfer efficiency as a function of expression level at fixed donor/acceptor ratio [43]. In the case of random interaction, the energy transfer between two fluorophores is linearly dependent on expression level and will diminish to zero at very low concentration of fluorophores. In the case of completely non-random interaction, the apparent FRET efficiency should be independent on concentration with an Ef_D intercept greater than zero. Fig. 7B shows Ef_D values measured in cells co-expressing WT-CFP/WT-YFP receptors and plotted as a function of estimated total concentration. The analysis revealed that a linear fit resulted in an Ef_D intercept at 0.13, confirming non-random interactions between the receptors. The fit also shows a slightly positive slope suggesting that in addition to the specific interactions, there is some contribution of random interaction to the measured Ef_D. Finally, two different types of analysis applied here confirm the specificity of 5-HT1A receptor oligomerization.

Another important aspect which may influence the specificity of receptor–receptor interaction is changes of 5-HT1A receptor/G_i-protein ratio in transfected cells. Although the expression level of 5-HT1A receptor in our experiments was similar to that obtained in hippocampus, the ratio between receptor and G_i-protein becomes significantly shifted from the "norm" value. This can lead to artificial oligomerization resulting from the competition of overabundant receptor for the limited copies of G-protein. To exclude such scenario, we analyzed oligomerization in the cells co-expressing wild-type or

Fig. 4. Acceptor-photobleaching FRET analysis of 5-HT1A oligomerization. (A) Confocal microscopy was used to visualize 5-HT1A-CFP and 5-HT1A-YFP co-expressed in the plasma membrane of N1E-115 cells. Fluorescence spectra were collected from a 2 µm optical slice and unmixed to CFP and YFP components using the Zeiss LSM510-Meta detector. The fluorescence image of the CFP channel (green), the YFP channel (red) and composite channel before and after bleaching are shown. The box 1 corresponds to the bleached regions of interest, while the box 2 corresponds to the non-bleached region of interest. Scale bar, 10 µm. (B) Enlargement of the box 1 is shown on the left. The 12-bit grayscale intensities of YFP [41] and CFP [41] during the whole trial are plotted for the bleached region of interest (right). (C) Enlargement of the box 2 is shown on the left. The 12-bit grayscale intensities of YFP [41] and CFP [41] during the whole trial are plotted for the non-bleached region of interest (right). (D) Apparent FRET efficiency Ef_D was calculated according to Eqs. (1) and (2). Data represent the means±S.E.M. from at least five independent experiments. Cells co- expressing cytosolic CFP and YFP were used as a negative control. A statistically significant difference between the FRET values obtained in cell co-expressing WT-CFP/WT-YFP and Mut- CFP/Mut-YFP or Mut-CFP/WT-YFP is indicated (**, $p<0.01$). Mut, acylation-deficient 5-HT1A mutant.

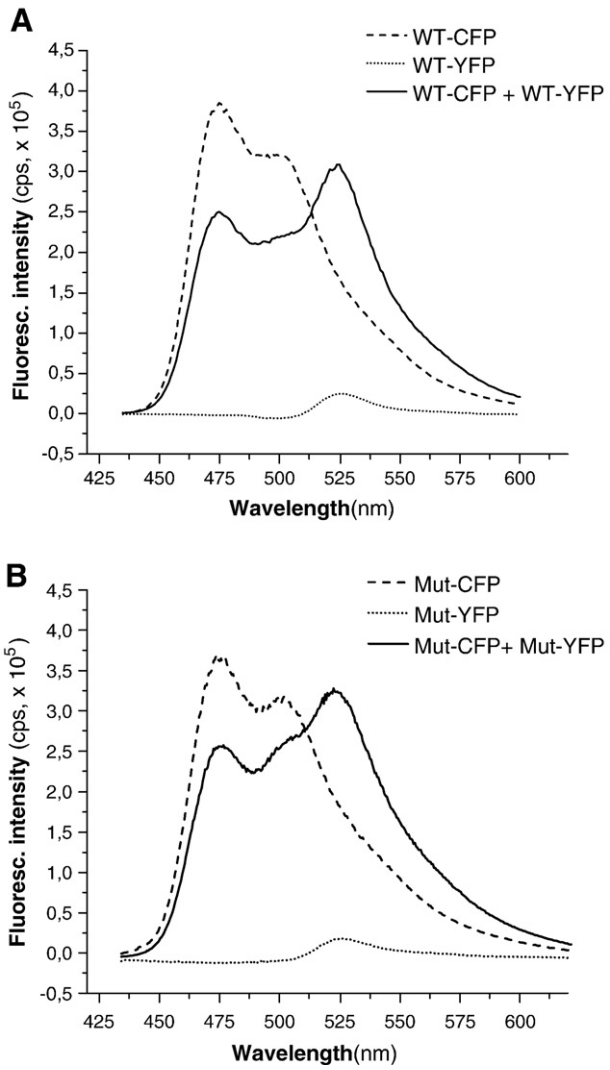

Fig. 6. Spectral analysis of living N1E-115 cells co-expressing CFP- and YFP-tagged 5-HT1A receptors. Fluorescence emission spectra of N1E-115 cells transfected with wild-type (A) or acylation-deficient (B) 5-HT1A receptors are shown. In both cases cells were transfected either with only CFP- (dashed line) or only with YFP-tagged (dotted line) receptors or were co-transfected with both YFP- and CFP-tagged receptors (solid line). Emission spectra were collected at excitation wavelength λ_{exc}=420 nm. Spectra were normalized to that obtained in cells transfected HA-tagged 5HT1A receptor. The data shown are representative of at least 3 independent experiments.

acylation-deficient receptor together with Gαi2, Gβ1 and Gγ2 subunits. Measurements of apparent FRET efficiency revealed that Ef_D values obtained after overexpression of G_i-protein fit perfectly to the curve shown in Fig. 7A (data not shown).

3.6. Quantitative analysis of oligomerization dynamics in living cells

To investigate the effect of receptor activation on 5-HT1A oligomerization, we applied a novel FRET approach named lux-FRET (linear unmixing of FRET spectral components) [41], which allows quantitative measurements of oligomerization during receptor stimulation with agonist. To evaluate time- and activation-correlated changes in receptor interaction, apparent FRET efficiencies measured from N1E-115 cells co-expressing 5-HT1A fusion proteins were monitored over time before and during incubation with agonist and/or antagonist. Cells were co-transfected with donor (5-HT1A-CFP) and acceptor (5-HT1A-YFP) proteins at a 1:1 ratio and emission spectra were recorded every 2 min using excitation wavelengths of 458 nm and 488 nm. For each time point, two quantities were determined, i.e. the product of characteristic FRET efficiency (E) and the fraction of donor participating in complexes (f_D) as well as the corresponding quantity describing the product of E and the fraction of acceptor participating in complexes (f_A). Both values characterize the stoichiometry of fluorescently labeled receptors and are used to verify the data obtained.

In the absence of receptor stimulation we obtained only slight fluctuations of Ef_D around the initial values in cells expressing wild-type 5-HT1A receptors. After treatment with serotonin at 10 μM, the values of Ef_D continuously decreased reaching a plateau after 10 min (Fig. 8A). In contrast, cells treated with PBS, did not show any significant changes of Ef_D values (Fig. 8A). The treatment of co-transfected cells with the selective 5-HT1A receptor antagonist, WAY100635 at 1 μM concentration blocked the agonist-mediated decrease of Ef_D (Fig. 8A). In order to quantify agonist-mediated changes of Ef_D, we chose a representative time point before adding serotonin (5 min before) and compared its value with that of a representative time point after agonist stimulation (15 min after 5-HT application) (Fig. 8B). This comparison revealed that stimulation of the 5-HT1A receptor with agonist results in a significant decrease of the Ef_D value by 12%±2.1%.

We also analyzed, whether the localization of receptor in lipid rafts may influence agonist-mediated decrease of Ef_D. Fig. 8B demonstrates that depletion of cholesterol by treatment of cells expressing wild-

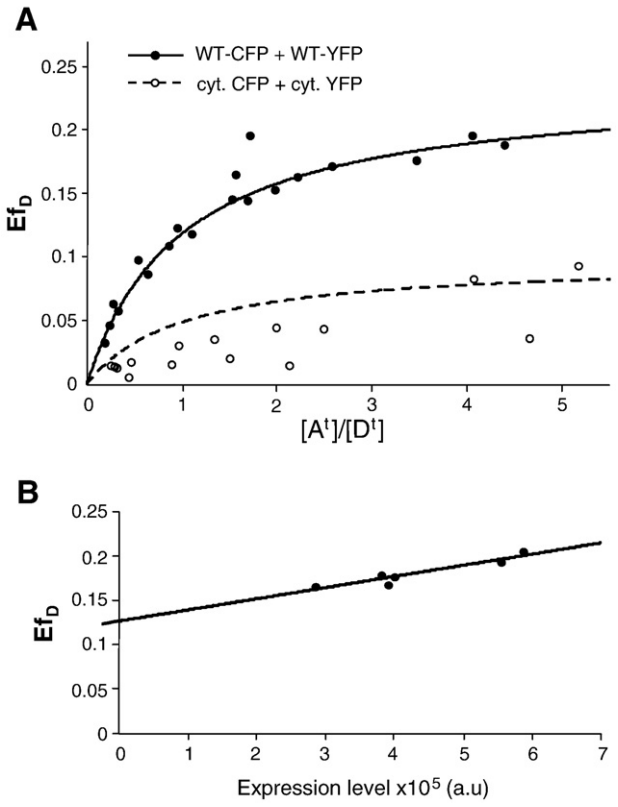

Fig. 7. Specificity of 5-HT1A receptor oligomerization. (A) Dependency of apparent FRET efficiency Ef_D on donor/acceptor ratio. 5-HT1A receptors labeled either with CFP [41] or YFP [41] were co-expressed at different ratios in N1E-115 cells, wherein the combined concentration of donors and acceptors was held constant. N1E-115 cells co-expressing cytosolic CFP and YFP were used as a control for random interactions. Emission spectra were obtained and analyzed as described in Material and Methods section. Ef_D values were calculated according to Eq. (3). and plotted against the $[A^t]/[D^t]$ ratio computed with Eq. (5). Data points were fitted according to Eq. (6). (B) Dependency of apparent FRET efficiency Ef_D on expression level at fixed donor to acceptor ratio. The Ef_D values were measured in cells co-expressing WT-CFP/WT-YFP receptors and plotted as a function of estimated total concentration. The data were collected from samples with a $[A^t]$ to $[D^t]$ ratio ranging between 8 and 10, and Ef_D values were calculated according to Eq. (3).

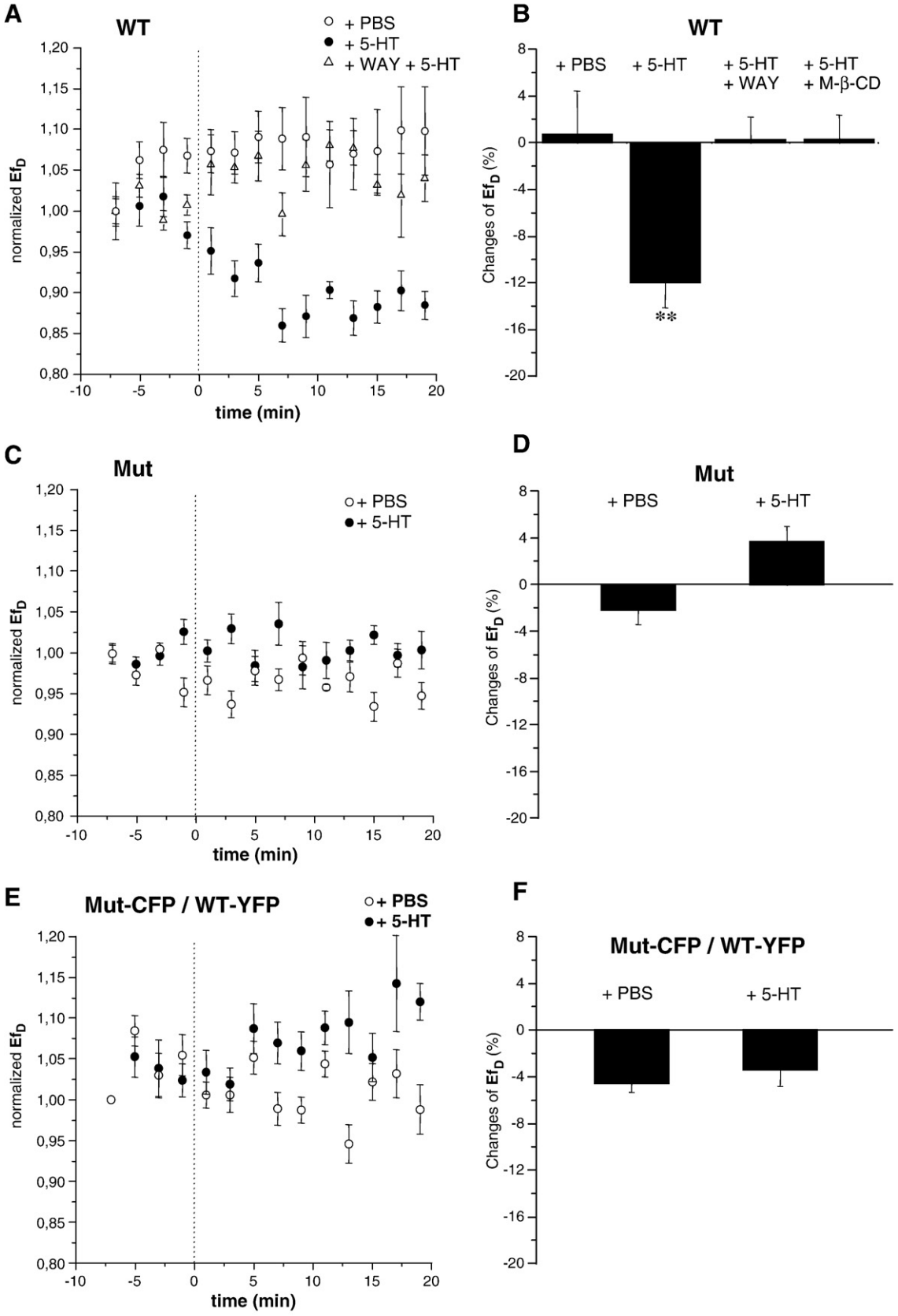

Fig. 8. Time course of FRET efficiency Ef_D upon receptor stimulation. The graphs on the left show the time course of Ef_D values calculated according to Eq. (1) for N1E-115 cells co-expressing WT-CFP/WT-YFP (A), Mut-CFP/Mut/YFP (C) or Mut-CFP/WT-YFP (E) receptors as FRET pairs. The cells were treated at zero time point with serotonin (10 μm), PBS, with serotonin together with WAY (1 μM) or with serotonin together with MßCD. All time-course values were normalized to unity at start for better visualization of differences. Data points represent mean ± S.E.M. ($n=6$). The graph on the right shows percentage of changes of apparent FRET efficiency (Ef_D) obtained 5 min before and 15 min after treatment for WT-CFP/WT-YFP (B), Mut- CFP/Mut-YFP (D) or Mut-CFP/WT-YFP (F). A statistically significant difference between values is noted (**, $p<0.01$).

type receptor with methyl-β-cyclodextrin abolished this effect, suggesting importance of lipid rafts for the agonist-mediated changes in receptor oligomerization.

Analysis of the time course of the apparent FRET efficiency in cells expressing acylation-deficient 5-HT1A receptor demonstrated that non-palmitoylated receptors do not produce any significant changes of Ef_D values after agonist stimulation (Fig. 8C and D). When the wild-type receptor was co-expressed with the acylation-deficient receptor, the agonist-mediated decrease of Ef_D value was also completely abolished, demonstrating the dominant-negative effect of non-palmitoylated receptor on the dynamic changes in receptor–receptor interactions (Fig. 8E and F).

We also performed a time-course analysis of Ef_A values for the wild-type and the acylation-deficient mutant. Similar to the results obtained for Ef_D, we observed a significant decrease of Ef_A values by 15.2%±2.9% after adding 10 μM serotonin to the cells expressing wild-type 5-HT1A receptors (Fig. S2). The Ef_A values obtained for the acylation-deficient receptor mutant as well as for the combination of wild-type and non-palmitoylated mutant were not affected by the agonist treatment (Fig. S2).

3.7. Agonist stimulation and lipid rafts localization of the 5-HT1A receptor

Results obtained in the present study suggested the importance of cholesterol-enriched membrane subdomains for receptor oligomerization (Figs. 3 and 8). Therefore, we compared the membrane distribution of the wild-type receptor before and after stimulation with agonist using density gradient centrifugation. N1E-115 cells expressing the 5-HT1A receptor were solubilized in cold Triton X-100 (TX-100) and subjected to centrifugation in Optiprep™ density gradient in order to isolate detergent- insoluble membrane fractions. Immunoblot analysis of gradient fractions revealed that 38%±7.8% (n=3) of the wild-type 5-HT1A receptor floated with the detergent-resistant low-density fractions along with the α_{i3}-subunit of heterotrimeric G-protein (Fig. 9). After treatment of cells with 10 μM of 5-HT, the yield of receptor in the light Triton X-100-resistant membrane fraction was not significantly changed and was found to be 34.6%±4.9% (n=3; Fig. 9). Chemical cross-linking performed before the TX-100 treatment and gradient centrifugation revealed that amount of receptor oligomers in lipid rafts was not changed upon agonist stimulation (data not shown). It is also notable

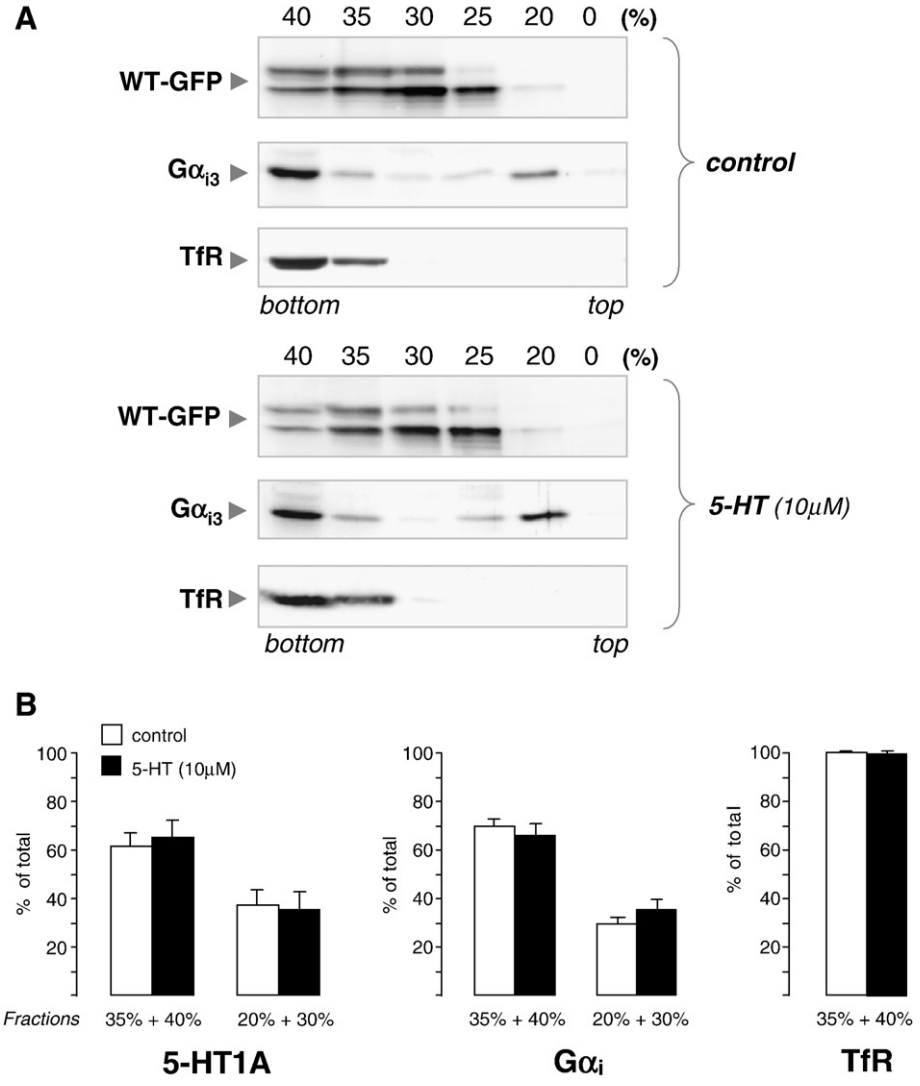

Fig. 9. Agonist stimulation does not change distribution of the 5-HT1A receptor in the detergent-resistant membrane fractions (DRMs). (A) The neuroblastoma N1E-115 cells expressing the wild-type 5-HT1A receptor fused to GFP were treated with 5-HT (10 μM) or PBS (control). Cells were lysed with cold 1% Triton-X100 and lysates were ultracentrifugated in an Optiprep™ density gradient. The gradient fractions were analyzed by immunoblotting. $G\alpha_i$ protein was used as DRM marker while transferrin receptor (TfR) was used as the non-DRM marker. (B) Relative amount of the 5-HT1A receptors, $G\alpha_i$ and transferrin receptor (TfR) in the high density fractions (35%+40%) and the buoyant low-density fractions (20%+30%) is shown. Quantitative analysis of the protein distribution was performed by densitometry and calculated in percentage of the total protein amount in all fractions. Data points represent mean±S.E.M. (n=3).

that distribution of the $G\alpha_{i3}$ protein and the transferrin receptor, which were used as rafts and non-rafts markers, respectively, did not change after agonist treatment (Fig. 9).

4. Discussion

During the last decade, a growing body of biochemical and biophysical evidence indicated that GPCRs can form oligomeric complexes. Although the existence of GPCR oligomers has now become generally accepted, their physiological incidence in native tissues as well as functional importance are still a matter of debate and in some cases remain even controversial [49,50]. It has been clearly documented that homo- and hetero-oligomerization of class C GPCRs such as metabotropic glutamate as well as $GABA_BB$ receptors is essential for the receptor trafficking to the cell surface, for ligand-induced receptor activation as well as for G-protein coupling [51,52]. In contrast, no general consensus is yet achieved for the functional importance of oligomerization for class A GPCRs. In the case of opioid receptor, heterodimers of kappa and delta receptors have been shown to form a distinct functional signaling unit *in vivo* [53]. Recent data on the heterodimerization between β1A and β2A receptors also demonstrated importance of oligomerization for the inhibition of agonist-promoted internalization of the β2A and its ability to activate the ERK1/2 MAPK signaling pathway [54]. On the other hand, β2A and rhodopsin receptors, which are often used as a model GPCRs for the homooligomerization analysis, can efficiently activate their G-proteins in monomeric conformation [55]. Similarly, oligomerization of the neurotensin NTS1 receptor is not required for G-protein activation, although it seems to alter the mode of the receptor-G protein interaction [56]. These findings show that receptor oligomerization plays differing functional roles at different receptor-G-protein interfaces, suggesting that there is no common function applicable to all GPCRs.

In the present study we verified the oligomerization state of the 5-HT1A receptor and also analyzed its oligomerization dynamics upon the agonist stimulation by using classical biochemical methods and different FRET-based approaches. In addition, we investigated the possible interplay between palmitoylation and oligomerization of the 5-HT1A receptor. A co-immunoprecipitation assay performed in neuroblastoma N1E-115 cells expressing receptor constructs containing different epitope tags revealed the presence of immunoreactive 5-HT1A receptors only in co-transfected cells and not in individually transfected cells mixed before cell lysis. This strongly suggests that the 5-HT1A receptor forms homo-oligomers. Homooligomerization of 5-HT1A receptors has been also previously reported for recombinant 5-HT1A receptor expressed in HEK-293 cells [57], suggesting that oligomerization is intrinsic to the 5-HT1A itself. In addition, oligomerization experiments using a plasma membrane impermeable cross-linker $BM[PEO]_3$ applied to intact cells showed that the predominant receptor species on the plasma membrane are homodimers.

Biochemical methods used in this study represent the classical approaches used for the detection of GPCR oligomerization. However, these methods require solubilization and concentration of the membrane proteins, which could possibly result in artificial aggregation of receptors [58]. In addition, these techniques do not allow an analysis of GPCR oligomerization dynamics in living cells. To overcome these limitations and to analyze the oligomerization behaviour of the 5-HT1A receptor in living cells, we applied different FRET-based approaches including the acceptor-photobleaching method [59], the fluorescence lifetime-based FRET measurement as well as a novel lux-FRET approach [41].

4.1. Verification of oligomerization specificity by a novel FRET-based approach

In addition to biochemical methods, we analyzed 5-HT1A receptor oligomerization by FRET using receptors fused to enhanced CFP or YFP as donor and acceptor, respectively. It is notable that CFP- and YFP-fused receptors demonstrated subcellular distribution, pharmacological profiles and signaling properties similar to that of their non-fluorescent wild-type or acylation-deficient counterparts [40] indicating that these fluorescent constructs can be used in functional studies.

By using both acceptor-photobleaching and the fluorescence lifetime FRET methods, we measured FRET between CFP- and YFP-tagged 5-HT1A receptors expressed at the surface of N1E-115 cells. A valid interpretation of FRET data is, however, not trivial because the FRET signal depends on several factors such as interaction affinity and stoichiometry of fusion proteins, their folding probability and their mutual orientation, [60,61]. Moreover, positive FRET signals may result not only from specific protein interactions including receptor oligomerization, but also from randomly distributed proteins, as may be the case after overexpression of donors and acceptors [62]. Based on critical analysis of BRET data, it has been recently considered that the contribution of non-specific interactions measured by resonance energy transfer may be even larger than previously thought [43]. Therefore, the analysis of FRET data over different donor to acceptor ratios and/or over different expression levels have been proposed as important prerequisite to discriminate between specific versus non-specific interaction [43].

Hence, using a novel lux-FRET approach, we obtained and analyzed apparent FRET efficiency as a function of the acceptor to donor ratio, $[A^t]/[D^t]$ with the aim to distinguish between these two cases (i.e. specific vs. non-specific interaction). By measuring the emission spectra at two different excitation wavelengths and applying linear unmixing, lux-FRET method allowed us to determine the stoichiometry of interacting fluorescently labeled receptors. Artifacts like bleed-through and cross-talk, which occur by using the filter channel based methods, do not affect such analysis. Moreover, this approach is more easily implemented than methods proposed previously [63,64]. Our data demonstrated that apparent FRET values obtained for different receptor combinations agreed with the model prediction for non-random interaction. In addition, the analysis of the energy transfer efficiency as a function of expression level at fixed donor to acceptor ratio demonstrates that FRET obtained for 5-HT1A receptors was largely independent of expression level. This observation further confirms specificity of oligomerization in case of the 5-HT1A receptor.

Further evidence for the specificity of 5-HT1A receptor oligomerization was obtained from the analysis of recently published data on receptor pharmacology [32]. The Hill coefficient value calculated for HA-tagged 5-HT1A receptor was found to be 0.50±0.17, which indicates negative cooperativity. According to the theory [65], the Hill coefficient value in negatively cooperating systems can be used to estimate the minimal number of receptor subunits in complex, and the Hill slope of 0.5 indicates that 5-HT1A exists as a dimer or higher-order oligomer.

4.2. Regulation of oligomerization by agonist; role of lipid rafts and receptor palmitoylation

In several biophysical studies investigating the effect of agonists on receptor oligomerization, changes in the resonance energy transfer were obtained after receptor stimulation [66]. This has often been interpreted as an agonist-induced change in oligomerization state. Since FRET efficiency highly depends on the relative distance and orientation between the donor and acceptor, such agonist- mediated changes in energy transfer may also reflect alterations in the pre-existing receptor conformation [67]. In the majority of studies, addition of agonist resulted in an increase of the FRET/BRET signal. However, agonist-dependent reduction of the signal has been reported for four GPCRs including cholecystokinin, neuropeptide Y4, thyrotropin TSH and somatostatin SSTR2 receptors [68–71]. Based on different tag combinations and positions (cholecystokinin receptor), on the FRAP technique (TSH receptor) as well as on biochemical analysis (neuropeptide Y4 and SSTR2 receptors), authors proposed

agonist-induced dissociation of oligomers rather than a conformational change as a possible reason for the decrease of the energy transfer efficiency. In the present study, we analyzed the time course of the apparent FRET efficiency for 5-HT1A receptor oligomerization and found that receptor stimulation with agonist leads to significant decrease of the FRET signal. On the other hand, the amount of 5-HT1A oligomers was not affected upon agonist stimulation as revealed by co-immunoprecipitation and cross-linking analysis. This result was in contrast to examples mentioned above and suggests that ligand-mediated decrease of FRET obtained for the 5-HT1A receptor does not arise from the dissociation of oligomers to monomers and is rather achieved by the conformational changes of pre-existing FRET-positive complexes to FRET-negative orientations.

A more intriguing finding was the dependence of 5-HT1A oligomerization efficiency and dynamics on the palmitoylation state of receptors. The results of the biophysical studies revealed that the removal of palmitoylation sites resulted in increased FRET efficiency. On the other hand, agonist-mediated decrease of FRET signal obtained for the wild-type receptor was completely abolished in cells expressing of acylation-deficient mutants. Combined with the fact that agonist stimulation does not change the amount of oligomers composed by non-palmitoylated receptor, this suggests that lack of palmitoylation does not directly affect the extent of oligomerization rather influences orientation of C-terminal CFP and YFP leading to increased FRET efficiency.

What could be a possible mechanism by which palmitoylation may influence oligomerization and functions of the 5-HT1A receptor? We have recently shown that a significant fraction of the 5-HT1A receptor resides in lipid rafts, while the non-acylated mutants (which also do not couple to G_i-proteins) are excluded from these membrane microdomains [32,40]. Based on these data in combination with results presented here, we propose the existence of two populations of 5-HT1A receptors. One population consists of receptor oligomers localized outside of lipid rafts. This population seems to be partly "non-functional" in terms of efficient signaling and needs raft localization to coincide with raft-resided G_i-proteins [72,73]. Another receptor population resides in lipid rafts and plays an important role in an efficient receptor-mediated signaling. This is also in line with the current view on the functional role of lipid rafts. Lipid rafts and caveolae have been shown to be involved in the regulation of various cell functions including the intracellular sorting of proteins and lipids [74], the establishment of cell polarity [74] and the fine tuning of signaling processes [75]. The detection of numerous signaling proteins within the detergent-resistant membrane fractions led to the assumption that lipid rafts represent scaffold platforms which facilitate signal transduction by spatially recruiting signaling components and by preventing an inappropriate cross-talk between pathways [76,77]. Several members of the serotonin receptor family, including 5-HT2A and 5-HT7 receptors have also been shown to be highly enriched in lipid rafts and caveolae [78,79], suggesting general importans of this membrane subdomains for the serotonergic signaling. Similar enrichment in lipid rafts/caveolae has also been reported for other member of GPCR superfamily, including GnRH, endothelin ET_B and ET_A and chemokine CCR5 receptors [80–83].

In the case of 5-HT1A receptor, stimulation with agonist results in changing FRET-positive to FRET-negative orientation of oligomers residing in lipid rafts. This may originate from a more tight association of palmitoylated receptor C-terminus with raft-specific lipids [84,85] or from increased coupling of receptor with raft-resided $G\alpha_i$ proteins, particularly upon agonist stimulation. Both raft as well as non-raft populations seem to exist in dynamic equilibrium, which is important for the fine tuning of receptor-mediated signaling. In this model palmitoylation does not directly modulate oligomerization of 5-HT1A, but rather serves as a targeting signal responsible for the retention of the 5-HT1A receptor in defined membrane microdomains. The fact that the FRET efficiency for the oligomers composed by wild-type receptors was lower than that for non-functional, acylation-deficient mutants is also in line with this model. Combined with the fact that cholesterol depletion resulted in the significant increase of FRET signal only in case of wild-type receptor, these data suggest that receptors residing in lipid rafts consist of oligomers in FRET-negative conformation. In addition, abolishing the agonist-mediated changes in the FRET efficiency obtained in cells expressing wild-type oligomers after cholesterol depletion further confirms the importance of lipid rafts in 5-HT1A-mediated signaling. Further experimentation will be necessary to validate this model and elucidate molecular mechanisms regulating interplay between palmitoylation and oligomerization.

Acknowledgments

These studies were supported by the fund of the Medical School at the University of Göttingen and by the Deutsche Forschungsgemeinschaft through the Center of Molecular Physiology of the Brain to E.G.P. and E.N., Grant PO 732 and a Georg Christoph Lichtenberg Stipend to A.W.

Appendix A. Supplementary data

Supplementary data associated with this article can be found, in the online version, at doi:10.1016/j.bbamcr.2008.02.021.

References

[1] L.A. Devi, Heterodimerization of G-protein-coupled receptors: pharmacology, signaling and trafficking, Trends Pharmacol. Sci. 22 (2001) 532.
[2] J.A. Javitch, The ants go marching two by two: oligomeric structure of G-protein-coupled receptors, Mol. Pharmacol. 66 (2004) 1077.
[3] R. Maggio, Z. Vogel, J. Wess, Coexpression studies with mutant muscarinic/adrenergic receptors provide evidence for intermolecular "cross-talk" between G-protein-linked receptors, Proc. Natl. Acad. Sci. U. S. A. 90 (1993) 3103.
[4] C. Monnot, C. Bihoreau, S. Conchon, K.M. Curnow, P. Corvol, E. Clauser, Polar residues in the transmembrane domains of the type 1 angiotensin II receptor are required for binding and coupling. Reconstitution of the binding site by co-expression of two deficient mutants, J. Biol. Chem. 271 (1996) 1507.
[5] Y. Liang, D. Fotiadis, S. Filipek, D.A. Saperstein, K. Palczewski, A. Engel, Organization of the G protein-coupled receptors rhodopsin and opsin in native membranes, J. Biol. Chem. 278 (2003) 21655.
[6] D. Salom, I. Le Trong, E. Pohl, J.A. Ballesteros, R.E. Stenkamp, K. Palczewski, D.T. Lodowski, Improvements in G protein-coupled receptor purification yield light stable rhodopsin crystals, J. Struct. Biol. 156 (2006) 497.
[7] M. Chabre, M. le Maire, Monomeric G-protein-coupled receptor as a functional unit, Biochemistry 44 (2005) 9395.
[8] S. Bulenger, S. Marullo, M. Bouvier, Emerging role of homo- and heterodimerization in G-protein-coupled receptor biosynthesis and maturation, Trends Pharmacol. Sci. 26 (2005) 131.
[9] K.A. Jones, B. Borowsky, J.A. Tamm, D.A. Craig, M.M. Durkin, M. Dai, W.J. Yao, M. Johnson, C. Gunwaldsen, L.Y. Huang, C. Tang, Q. Shen, J.A. Salon, K. Morse, T. Laz, K.E. Smith, D. Nagarathnam, S.A. Noble, T.A. Branchek, C. Gerald, GABA(B) receptors function as a heteromeric assembly of the subunits GABA(B)R1 and GABA(B)R2, Nature 396 (1998) 674.
[10] K. Kaupmann, B. Malitschek, V. Schuler, J. Heid, W. Froestl, P. Beck, J. Mosbacher, S. Bischoff, A. Kulik, R. Shigemoto, A. Karschin, B. Bettler, GABA(B)-receptor subtypes assemble into functional heteromeric complexes, Nature 396 (1998) 683.
[11] J.H. White, A. Wise, M.J. Main, A. Green, N.J. Fraser, G.H. Disney, A.A. Barnes, P. Emson, S.M. Foord, F.H. Marshall, Heterodimerization is required for the formation of a functional GABA(B) receptor, Nature 396 (1998) 679.
[12] S. Angers, A. Salahpour, M. Bouvier, Dimerization: an emerging concept for G protein- coupled receptor ontogeny and function, Annu. Rev. Pharmacol. Toxicol. 42 (2002) 409.
[13] K.D. Pfleger, K.A. Eidne, Monitoring the formation of dynamic G-protein-coupled receptor-protein complexes in living cells, Biochem. J. 385 (2005) 625.
[14] R.M. Siegel, F.K. Chan, D.A. Zacharias, R. Swofford, K.L. Holmes, R.Y. Tsien, M.J. Lenardo, Measurement of molecular interactions in living cells by fluorescence resonance energy transfer between variants of the green fluorescent protein, Sci. STKE 2000 (2000) L1.
[15] J.R. Lakowicz, Principles of Fluorescence Spectroscopy, Springer, 2006.
[16] P.R. Albert, Heterologous expression of G protein-linked receptors in pituitary and fibroblast cell lines, Vitam. Horm. 48 (1994) 59.
[17] N.M. Barnes, T. Sharp, A review of central 5-HT receptors and their function, Neuropharmacology 38 (1999) 1083.
[18] J.R. Raymond, Y.V. Mukhin, T.W. Gettys, M.N. Garnovskaya, The recombinant 5- HT1A receptor: G protein coupling and signalling pathways, Br. J. Pharmacol. 127 (1999) 1751.
[19] R. Andrade, R.C. Malenka, R.A. Nicoll, A G protein couples serotonin and GABAB receptors to the same channels in hippocampus, Science 234 (1986) 1261.

[20] W.P. Clarke, F.D. Yocca, S. Maayani, Lack of 5-hydroxytryptamine1A-mediated inhibition of adenylyl cyclase in dorsal raphe of male and female rats, J. Pharmacol. Exp. Ther. 277 (1996) 1259.
[21] A. Fargin, J.R. Raymond, J.W. Regan, S. Cotecchia, R.J. Lefkowitz, M.G. Caron, Effector coupling mechanisms of the cloned 5-HT1A receptor, J. Biol. Chem. 264 (1989) 14848.
[22] M.N. Garnovskaya, T. van Biesen, B. Hawe, R.S. Casanas, R.J. Lefkowitz, J.R. Raymond, Ras-dependent activation of fibroblast mitogen-activated protein kinase by 5-HT1A receptor via a G protein beta gamma-subunit-initiated pathway, Biochemistry 35 (1996) 13716.
[23] J.J. Radley, B.L. Jacobs, 5-HT1A receptor antagonist administration decreases cell proliferation in the dentate gyrus, Brain Res. 955 (2002) 264.
[24] T. Manzke, U. Guenther, E.G. Ponimaskin, M. Haller, M. Dutschmann, S. Schwarzacher, D.W. Richter, 5-HT4(a) receptors avert opioid-induced breathing depression without loss of analgesia, Science 301 (2003) 226.
[25] D.W. Richter, T. Manzke, B. Wilken, E. Ponimaskin, Serotonin receptors: guardians of stable breathing, Trends Mol. Med. 9 (2003) 542.
[26] P.R. Saxena, C.M. Villalon, Brain 5-HT1A receptor agonism: a novel mechanism for antihypertensive action, Trends Pharmacol. Sci. 11 (1990) 95.
[27] P.W. Burnet, I.N. Mefford, C.C. Smith, P.W. Gold, E.M. Sternberg, Hippocampal 5- HT1A receptor binding site densities, 5-HT1A receptor messenger ribonucleic acid abundance and serotonin levels parallel the activity of the hypothalamo-pituitary-adrenal axis in rats, Behav. Brain Res. 73 (1996) 365.
[28] D.H. Overstreet, Behavioral characteristics of rat lines selected for differential hypothermic responses to cholinergic or serotonergic agonists, Behav. Genet. 32 (2002) 335.
[29] B. Bjorvatn, R. Ursin, Changes in sleep and wakefulness following 5-HT1A ligands given systemically and locally in different brain regions, Rev. Neurosci. 9 (1998) 265.
[30] J.A. Gordon, R. Hen, The serotonergic system and anxiety, Neuromolecular. Med. 5 (2004) 27.
[31] C.L. Parks, P.S. Robinson, E. Sibille, T. Shenk, M. Toth, Increased anxiety of mice lacking the serotonin1A receptor, Proc. Natl. Acad. Sci. U. S. A. 95 (1998) 10734.
[32] E. Papoucheva, A. Dumuis, M. Sebben, D.W. Richter, E.G. Ponimaskin, The 5-hydroxytryptamine(1A) receptor is stably palmitoylated, and acylation is critical for communication of receptor with Gi protein, J. Biol. Chem. 279 (2004) 3280.
[33] R. Qanbar, M. Bouvier, Role of palmitoylation/depalmitoylation reactions in G-protein- coupled receptor function, Pharmacol. Ther. 97 (2003) 1.
[34] J.G. Mulheron, S.J. Casanas, J.M. Arthur, M.N. Garnovskaya, T.W. Gettys, J.R. Raymond, Human 5-HT1A receptor expressed in insect cells activates endogenous G(o)-like G protein(s), J. Biol. Chem. 269 (1994) 12954.
[35] S. Moffett, B. Mouillac, H. Bonin, M. Bouvier, Altered phosphorylation and desensitization patterns of a human beta 2-adrenergic receptor lacking the palmitoylated Cys341, EMBO J. 12 (1993) 349.
[36] B.F. O'Dowd, M. Hnatowich, M.G. Caron, R.J. Lefkowitz, M. Bouvier, Palmitoylation of the human beta 2-adrenergic receptor. Mutation of Cys341 in the carboxyl tail leads to an uncoupled nonpalmitoylated form of the receptor, J. Biol. Chem. 264 (1989) 7564.
[37] Y. Okamoto, H. Ninomiya, M. Tanioka, A. Sakamoto, S. Miwa, T. Masaki, Cysteine residues in the carboxyl terminal domain of the endothelin-B receptor are required for coupling with G-proteins, J. Cardiovasc. Pharmacol. 31 (Suppl. 1) (1998) S230–S232.
[38] C. Blanpain, V. Wittamer, J.M. Vanderwinden, A. Boom, B. Renneboog, B. Lee, E. Le Poul, L. El Asmar, C. Govaerts, G. Vassart, R.W. Doms, M. Parmentier, Palmitoylation of CCR5 is critical for receptor trafficking and efficient activation of intracellular signaling pathways, J. Biol. Chem. 276 (2001) 23795.
[39] S.M. Miggin, O.A. Lawler, B.T. Kinsella, Palmitoylation of the human prostacyclin receptor. Functional implications of palmitoylation and isoprenylation, J. Biol. Chem. 278 (2003) 6947.
[40] U. Renner, K. Glebov, T. Lang, E. Papusheva, S. Balakrishnan, B. Keller, D.W. Richter, R. Jahn, E. Ponimaskin, Localization of the mouse 5-hydroxytryptamine(1A) receptor in lipid microdomains depends on its palmitoylation and is involved in receptor-mediated signaling, Mol. Pharmacol. 72 (2007) 502.
[41] J. Wlodarczyk, A. Woehler, F. Kobe, E. Ponimaskin, A. Zeug, E. Neher, Analysis of FRET-signals in the presence of free donors and acceptors, Biophys. J. 94 (2008) 986.
[42] W. Veatch, L. Stryer, The dimeric nature of the gramicidin A transmembrane channel: conductance and fluorescence energy transfer studies of hybrid channels, J. Mol. Biol. 113 (1977) 89.
[43] J.R. James, M.I. Oliveira, A.M. Carmo, A. Iaboni, S.J. Davis, A rigorous experimental framework for detecting protein oligomerization using bioluminescence resonance energy transfer, Nat. Methods 3 (2006) 1001.
[44] D. Hoyer, A. Pazos, A. Probst, J.M. Palacios, Serotonin receptors in the human brain. I. Characterization and autoradiographic localization of 5-HT1A recognition sites. Apparent absence of 5-HT1B recognition sites, Brain Res. 376 (1986) 85.
[45] A. Pazos, J.M. Palacios, Quantitative autoradiographic mapping of serotonin receptors in the rat brain. I. Serotonin-1 receptors, Brain Res. 346 (1985) 205.
[46] T. Harder, P. Scheiffele, P. Verkade, K. Simons, Lipid domain structure of the plasma membrane revealed by patching of membrane components, J. Cell Biol. 141 (1998) 929.
[47] K. Herrick-Davis, E. Grinde, J.E. Mazurkiewicz, Biochemical and biophysical characterization of serotonin 5-HT2C receptor homodimers on the plasma membrane of living cells, Biochemistry 43 (2004) 13963.
[48] K. Herrick-Davis, E. Grinde, T.J. Harrigan, J.E. Mazurkiewicz, Inhibition of serotonin 5- hydroxytryptamine2c receptor function through heterodimerization: receptor dimmers bind two molecules of ligand and one G-protein, J. Biol. Chem. 280 (2005) 40144.
[49] R. Maggio, F. Novi, M. Scarselli, G.U. Corsini, The impact of G-protein-coupled receptor hetero-oligomerization on function and pharmacology, FEBS J. 272 (2005) 2939.
[50] G. Milligan, G-protein-coupled receptor heterodimers: pharmacology, function and relevance to drug discovery, Drug Discov. Today 11 (2006) 541.
[51] M. Bouvier, Oligomerization of G-protein-coupled transmitter receptors, Nat. Rev., Neurosci. 2 (2001) 274.
[52] J.P. Pin, T. Galvez, L. Prezeau, Evolution, structure, and activation mechanism of family 3/C G-protein-coupled receptors, Pharmacol. Ther. 98 (2003) 325.
[53] M. Waldhoer, J. Fong, R.M. Jones, M.M. Lunzer, S.K. Sharma, E. Kostenis, P.S. Portoghese, J.L. Whistler, A heterodimer-selective agonist shows in vivo relevance of G protein-coupled receptor dimers, Proc. Natl. Acad. Sci. U. S. A. 102 (2005) 9050.
[54] C. Lavoie, J.F. Mercier, A. Salahpour, D. Umapathy, A. Breit, L.R. Villeneuve, W.Z. Zhu, R.P. Xiao, E.G. Lakatta, M. Bouvier, T.E. Hebert, Beta 1/beta 2-adrenergic receptor heterodimerization regulates beta 2-adrenergic receptor internalization and ERK signaling efficacy, J. Biol. Chem. 277 (2002) 35402.
[55] M.R. Whorton, M.P. Bokoch, S.G. Rasmussen, B. Huang, R.N. Zare, B. Kobilka, R.K. Sunahara, A monomeric G protein-coupled receptor isolated in a high-density lipoprotein particle efficiently activates its G protein, Proc. Natl. Acad. Sci. U. S. A. 104 (2007) 7682.
[56] J.F. White, J. Grodnitzky, J.M. Louis, L.B. Trinh, J. Shiloach, J. Gutierrez, J.K. Northup, R. Grisshammer, Dimerization of the class A G protein-coupled neurotensin receptor NTS1 alters G protein interaction, Proc. Natl. Acad. Sci. U. S. A. 104 (2007) 12199.
[57] K. Salim, T. Fenton, J. Bacha, H. Urien-Rodriguez, T. Bonnert, H.A. Skynner, E. Watts, J. Kerby, A. Heald, M. Beer, G. McAllister, P.C. Guest, Oligomerization of G- protein-coupled receptors shown by selective co-immunoprecipitation, J. Biol. Chem. 277 (2002) 15482.
[58] C. Harrison, P.H. van der Graaf, Current methods used to investigate G protein coupled receptor oligomerisation, J. Pharmacol. Toxicol. Methods 54 (2006) 26.
[59] P.I. Bastiaens, I.V. Majoul, P.J. Verveer, H.D. Soling, T.M. Jovin, Imaging the intracellular trafficking and state of the AB5 quaternary structure of cholera toxin, EMBO J. 15 (1996) 4246.
[60] A.K. Kenworthy, M. Edidin, Distribution of a glycosylphosphatidylinositol-anchored protein at the apical surface of MDCK cells examined at a resolution of <100 A using imaging fluorescence resonance energy transfer, J. Cell Biol. 142 (1998) 69.
[61] H. Wallrabe, M. Elangovan, A. Burchard, A. Periasamy, M. Barroso, Confocal FRET microscopy to measure clustering of ligand-receptor complexes in endocytic membranes, Biophys. J. 85 (2003) 559.
[62] B.H. Meyer, J.M. Segura, K.L. Martinez, R. Hovius, N. George, K. Johnsson, H. Vogel, FRET imaging reveals that functional neurokinin-1 receptors are monomeric and reside in membrane microdomains of live cells, Proc. Natl. Acad. Sci. U. S. A. 103 (2006) 2138.
[63] A. Hoppe, K. Christensen, J.A. Swanson, Fluorescence resonance energy transfer-based stoichiometry in living cells, Biophys. J. 83 (2002) 3652.
[64] T. Zal, N.R. Gascoigne, Using live FRET imaging to reveal early protein-protein interactions during T cell activation, Curr. Opin. Immunol. 16 (2004) 674.
[65] H. Abeliovich, An empirical extremum principle for the hill coefficient in ligand-protein interactions showing negative cooperativity, Biophys. J. 89 (2005) 76.
[66] S. Terrillon, M. Bouvier, Roles of G-protein-coupled receptor dimerization, EMBO Rep. 5 (2004) 30.
[67] C. Hoffmann, G. Gaietta, M. Bunemann, S.R. Adams, S. Oberdorff-Maass, B. Behr, J.P. Vilardaga, R.Y. Tsien, M.H. Ellisman, M.J. Lohse, A FlAsH-based FRET approach to determine G protein-coupled receptor activation in living cells, Nat. Methods 2 (2005) 171.
[68] M.M. Berglund, D.A. Schober, M.A. Statnick, P.H. McDonald, D.R. Gehlert, The use of bioluminescence resonance energy transfer 2 to study neuropeptide Y receptor agonist-induced beta-arrestin 2 interaction, J. Pharmacol. Exp. Ther. 306 (2003) 147.
[69] G.A. Grant, Z. Hu, X.L. Xu, Hybrid tetramers reveal elements of cooperativity in Escherichia coli D-3-phosphoglycerate dehydrogenase, J. Biol. Chem. 278 (2003) 18170.
[70] Z.J. Cheng, L.J. Miller, Agonist-dependent dissociation of oligomeric complexes of G protein-coupled cholecystokinin receptors demonstrated in living cells using bioluminescence resonance energy transfer, J. Biol. Chem. 276 (2001) 48040.
[71] K.M. Kroeger, A.C. Hanyaloglu, R.M. Seeber, L.E. Miles, K.A. Eidne, Constitutive and agonist-dependent homo-oligomerization of the thyrotropin-releasing hormone receptor. Detection in living cells using bioluminescence resonance energy transfer, J. Biol. Chem. 276 (2001) 12736.
[72] M.B. Emerit, S. el Mestikawy, H. Gozlan, B. Rouot, M. Hamon, Physical evidence of the coupling of solubilized 5-HT1A binding sites with G regulatory proteins, Biochem. Pharmacol. 39 (1990) 7.
[73] P. Oh, J.E. Schnitzer, Segregation of heterotrimeric G proteins in cell surface microdomains. G(q) binds caveolin to concentrate in caveolae, whereas G(i) and G(s) target lipid rafts by default, Mol. Biol. Cell 12 (2001) 685.
[74] H. Sprong, S.P. van der, G. van Meer, How proteins move lipids and lipids move proteins, Nat. Rev., Mol. Cell Biol. 2 (2001) 504.
[75] D. Toomre, J.A. Steyer, P. Keller, W. Almers, K. Simons, Fusion of constitutive membrane traffic with the cell surface observed by evanescent wave microscopy, J. Cell Biol. 149 (2000) 33.
[76] L.J. Foster, C.L. De Hoog, M. Mann, Unbiased quantitative proteomics of lipid rafts reveals high specificity for signaling factors, Proc. Natl. Acad. Sci. U. S. A. 100 (2003) 5813.
[77] T. Okamoto, A. Schlegel, P.E. Scherer, M.P. Lisanti, Caveolins, a family of scaffolding proteins for organizing "preassembled signaling complexes" at the plasma membrane, J. Biol. Chem. 273 (1998) 5419.

[78] A. Bhatnagar, D.J. Sheffler, W.K. Kroeze, B. Compton-Toth, B.L. Roth, Caveolin-1 interacts with 5-HT2A serotonin receptors and profoundly modulates the signaling of selected Galphaq-coupled protein receptors, J. Biol. Chem. 279 (2004) 34614.
[79] B. Sjogren, P. Svenningsson, Caveolin-1 affects serotonin binding and cell surface levels of human 5-HT7(a) receptors, FEBS Lett. 581 (2007) 5115.
[80] T. Yamaguchi, Y. Murata, Y. Fujiyoshi, T. Doi, Regulated interaction of endothelin B receptor with caveolin-1, Eur. J. Biochem. 270 (2003) 1816.
[81] Y. Okamoto, H. Ninomiya, S. Miwa, T. Masaki, Cholesterol oxidation switches the internalization pathway of endothelin receptor type A from caveolae to clathrin-coated pits in Chinese hamster ovary cells, J. Biol. Chem. 275 (2000) 6439.
[82] Y. Percherancier, B. Lagane, T. Planchenault, I. Staropoli, R. Altmeyer, J.L. Virelizier, F. Arenzana-Seisdedos, D.C. Hoessli, F. Bachelerie, HIV-1 entry into T-cells is not dependent on CD4 and CCR5 localization to sphingolipid-enriched, detergent-resistant, raft membrane domains, J. Biol. Chem. 278 (2003) 3153.
[83] B. Chini, M. Parenti, G-protein coupled receptors in lipid rafts and caveolae: how, when and why do they go there? J. Mol. Endocrinol. 32 (2004) 325.
[84] K.A. Melkonian, A.G. Ostermeyer, J.Z. Chen, M.G. Roth, D.A. Brown, Role of lipid modifications in targeting proteins to detergent-resistant membrane rafts. Many raft proteins are acylated, while few are prenylated, J. Biol. Chem. 274 (1999) 3910.
[85] S. Moffett, D.A. Brown, M.E. Linder, Lipid-dependent targeting of G proteins into rafts, J. Biol. Chem. 275 (2000) 2191.